Bioelectrocatalytic endpoint assays based on steady-state diffusion current at microelectrode array

Tatsuo Noda, Katsumi Hamamoto, Maiko Tsutsumi, Seiya Tsujimura, Osamu Shirai, and Kenji Kano*

Division of Applied Life Sciences, Graduate School of Agriculture, Kyoto University, Sakyo, Kyoto 606-8502, Japan

*Corresponding author: Tel: +81-75-753-6392; fax: +81-75-753-6456; E-mail: kkano@kais.kyoto-u.ac.jp

Abstract

Highly reproducible bioelectrocatalytic endpoint assays are described. The method is based on a complete redox conversion of a substrate to a redox mediator with a corresponding redox enzyme and an amperometric detection of the reduced mediator on a diffusionally independent microelectrode array. The current reaches a steady state within a few seconds and is proportional to the number of the integrated microelectrodes. The method has successfully been applied to histamine detection at micro-molar level and glucose detection at milli-molar level.

Keywords: Bioelectrocatalysis, Endpoint assay, Microelectrode array, Histamine assay, Glucose assay

1. Introduction

Electrochemical analysis with biological functions such as biosensors have been received much attention in the field of clinical analysis, food industry and environmental monitoring, hence numerous efforts have been devoted to develop rapid, reliable and accurate electrochemical biosensors [1]. However, most of the conventional amperometric biosensors have an intrinsic disadvantage in the issue that the response current is liable to be affected by either enzyme kinetic-related factor or diffusion-related factor of substrate (and mediator in mediated bioelectrocatalysis) [2]. This issue is frequently addressed by using permeable membrane-coated electrodes with raised enzyme activity under convectional conditions [3]. However, it is difficult to strictly control the permeability of membranes on miniaturized biosensors and to realize high reproducibility. Coulometry as an absolute quantitative analysis is an alternative of bio-sensing [4, 5], but is often time-consuming.

Spherical diffusion plays an important role at microelectrode and provides steady-state current even under quiescent conditions [6]. In our best knowledge, however, there is no report on micro-biosensors utilizing such spherical diffusion. One of the reasons is that the current is usually within or below nano-ampere range, which might not be convenient for practical use. Microelectrode array (MEA) is designed by integration of several microelectrodes to increase the current intensity in various amperometric sensors [7–11]. In MEAs, the distance between microdisc electrodes should be larger than 12 times of the radius (r) in order to ensure diffusional independence of the microelectrodes [12], although the geometry and the shape of microelectrodes are important factors determining the timescale [9–11]. It is not easy to fabricate such ideal MEAs, and diffusion-layer overlapping seems to occur at most of MEAs. The other reason is that sufficiently high enzyme activity is required to satisfy the diffusion-controlled condition of substrate in bioelectrocatalytic reactions.

Herein, we describe a reproducible amperometric detection method by monitoring steady-state diffusion current in mediated bioelectrocatalysis. First, we will propose a fabrication method of an diffusionally independent MEA. In addition, the endpoint method was incorporated in order to eliminate the effect of enzyme activity change and to increase the applicability of the method in practical bioassays, where the electron equivalent of substrate is completely transferred to that of mediator with the aid of redox enzyme in solution. The concentration of the reduced mediator (for the oxidation of substrate) is determined from the steady-state current at the MEA. The amperometric endpoint assays were applied to determining histamine at micro-molar level with histamine dehydrogenase (HmDH) and ferricyanide (as a mediator) and glucose at milli-molar level with pyrroloquinoline quinone (PQQ)-dependent glucose dehydrogenase (PQQ-GDH) and benzoquinone (as a mediator). The performance will be discussed in detail.

2. Experimental

2.1. Reagents and materials

Recombinant HmDH was expressed in *Escherichia coli* and purified as described previously [13]. The protein concentration was determined using a modified Lowry method with a DC Protein Assay Kit (Bio-Rad, USA) with bovine serum albumin as a standard protein. PQQ-GDH (EC 1.1.5.2 4200 U mg^{-1}) was obtained from Amano Enzyme (Japan). Mutarotase (EC 5.1.3.3 913 U mL^{-1}) was purchased from Oriental Yeast (Japan). All other chemicals were of analytical reagent grade and were used without further purification. D-Glucose stock solution was prepared with a phosphate buffer (0.1 M, pH 7) and stored overnight to reach the mutarotative equilibrium. Epoxy resin (Alardite 2020) and silver-epoxy resin (Dotite D-753) were obtained from Huntsman (USA) and Fujikura Kasei (Japan), respectively.

74

75 *2.2. Fabrication of microelectrode array (MEA)*

76 The fabrication scheme and the structure of our MEA are illustrated in Fig. 1. Firstly, a Pt
77 wire (20 μm in diameter; Niraco, Japan) was inserted into a silicon tube (i.d. 0.5 mm). The tube
78 was filled half with the epoxy resin (overnight, 55 ºC). The silver-epoxy resin was crammed into
79 the tube from the opposite side (4 h, 55 ºC). The resin was ejected from the silicon tube and is
80 called Pt-embedded rod. A blank rod was also prepared in the same manner without using Pt
81 wire. The Pt-embedded rods and the blank rods were inserted together in a silicon tube (i.d. 3
82 mm) (Fig. 1a). The Pt-embedded rods were arrayed to keep away from the neighboring ones in a
83 distance between the Pt wires of at least 500 μm (Fig. 1b). The number of the Pt-embedded rod
84 in the MEA (N) was varied from 1 to 7. In this paper, a single microelectrode is described as
85 MEA with N = 1, for simplification in description. After arraying the rods, the space among the
86 rods was filled with the epoxy resin. The rod array was then ejected from the silicon tube and
87 mounted in a glass tube (i.d. 3 mm). The silver-epoxy resin was crammed into the glass tube
88 from the opposite side and a lead wire was inserted in the silver-epoxy resin for the electrical
89 connect with the Pt-embedded rods. The glass tube was filled with the epoxy resin in the back
90 side (Fig. 1c). The surface of the MEA was polished to a flat and mirror finish with sandpaper
91 (#1500) and alumina slurry (0.05 μm).

92

93 *2.3. Electrochemical measurements and endpoint assays of histamine and glucose with MEA*

94 Cyclic voltammetry and amperometry were carried out in a three-electrode system on an
95 ALS CHI 611B electrochemical analyzer (BAS Inc.) equipped with a faraday gage in a
96 laboratory-made electrolysis cell at a total volume of 1.0 mL. The MEA, a Pt wire and an
97 Ag|AgCl|KCl (sat.) were used as the working, counter and reference electrodes, respectively. All
98 potentials in this paper are referred to the reference electrode. The total volume of the analytical

solution was 1.0 mL.

In histamine detection, 10 μL of a histamine sample solution was added to 1.0 mL of 0.1 M phosphate buffer (pH 7.0) containing 500 nM HmDH and 5 mM $K_3[Fe(CN)_6]$. After incubation at room temperature for 20 min, the amperometric detection was performed at +0.6 V. In glucose detection, 100 μL of a glucose sample solution was added to 1.0 mL of 30 mM MOPS buffer (pH 7.0) containing 21 U PQQ-GDH, 9 U mutarotase, 25 mM benzoquinone and 3 mM $CaCl_2$. After incubation at room temperature for 15 min under anaerobic conditions with Ar, the amperometric detection was performed at +0.85 V under quiescent conditions.

3. Results and discussion

3.1. Characterization of the MEA

All of the MEAs (N = 1, 3, 7) showed typical sigmoidal steady-state shape for $[Fe(CN)_6]^{3-}$ at 20 mV s^{-1} and the current was proportional to N (Fig. 2). Such sigmoidal response was observed at scan rates of 5–100 mV s^{-1} and was independent of the scan rate. These results support that the steady-state spherical diffusion layer of each microelectrode is not overlapped with that of the adjacent ones. The steady-state limiting current (i_{lim}) is given by:

$$i_{lim} = 4NnFrDc \quad (1)$$

where n, D, and c are the number of electron, diffusion coefficient, and the bulk concentration of analyte, respectively. F is the Faraday constant. Thus, once NrD is determined experimentally with a given MEA, c can be easily evaluated from $i_{lim.}$. In potential-step chronoamperometry, the current reached into almost steady state within 2 s, as shown in the inset of Fig. 2. In the following, the current after 5 s was taken as i_{lim}.

3.2. Responses to histamine at the MEA

Histamine analysis is one of the major concerns in clinical and food chemistry because histamine is a transmitter in the nervous system and a powerful biological marker of food freshness [14, 15]. HmDH catalyzes a 2-electon oxidation of histamine to give imidazole acetaldehyde [16]. Several redox compounds such as $[Fe(CN)_6]^{3-}$ and osmium (III) complexes work as electron acceptors of the reduced HmDH [17, 18]. In addition, the product imidazole acetaldehyde is proposed to be oxidized non-enzymatically to imidazole acetate by some electron acceptor in solution [17]. When $[Fe(CN)_6]^{3-}$ was used as an electron acceptor, the overall reaction is expected as follows.

$$\text{histamine} + 4\,[Fe(CN)_6]^{3-} + 2H_2O \rightarrow \text{imidazole acetate} + 4\,[Fe(CN)_6]^{4-} + NH_3 + 4H^+ \quad (2)$$

The succeeding non-enzymatic 2-electron oxidation will increase sensitivity twice in the histamine determination.

The i_{lim} of $[Fe(CN)_6]^{4-}$ in the endpoint assay detection with the MEA (N = 7) was in a very nice linear correlation to c(histamine) with a correlation coefficient larger than 0.999 over a wide range of c(histamine) from 10 to 1000 μM. The detection limit was 8.0 μM at an S/N ratio of 3, which is higher than some reported works [17–20]. In addition, the detection limit can be improved by increasing the number of embedded microelectrodes [7]. The relative standard deviation was 4.1% for five separate measurements at 10 μM histamine, in which the MEA surface was polished with alumina slurry before each measurement. The sensitivity ($4NnFrD$) was 6.6×10^{-2} A M^{-1} for N = 7 and was proportional to N (2.9×10^{-2} A M^{-1} for N = 3 and 9.2×10^{-3} A M^{-1} for N = 1). From the result, the averaged $4nFrD$ value is evaluated as 9.5×10^{-3} A M^{-1} for the histamine analysis with the MEA. In a separate experiment, the $4FrD$ value of $[Fe(CN)_6]^{4-}$ was evaluated as 2.4×10^{-3} A M^{-1} at the MEA in 0.1 M phosphate buffer (pH 7.0). The comparison of the two values can verify our expectation that n = 4 (Eq. 2).

3.3. Responses to glucose at the MEA

Metabolic disorders like diabetes mellitus are reflected by human blood glucose concentrations higher or lower than the normal range of 4.4–6.6 mM [21]. When we apply our amperometric endpoint assay to such high concentrations of the analyte, very fast enzymatic conversion is required. PQQ-GDH catalyzes the 2-electron oxidation of β-D-glucose with several artificial electron acceptors. The activity is very high [22]. From the kinetic viewpoint, we selected *p*-benzoquinone as an electron acceptor in the PQQ-GDH reaction [23]. The overall reaction is written by:

β-D-glucose + *p*-benzoquinone → gluconolactone + hydroquinone (3)

We first tried to amperometric trace of the enzyme kinetics by measuring time dependence of i_{lim} of hydroquinone generated in the reaction of Eq. (3). The PQQ-GDH reaction appeared to reach an endpoint within 15 min under the present conditions, but i_{lim} was gradually increasing after 15 min. This is due to the mutarotation. Therefore, it is essential to accelerate the mutarotation proceeding simultaneously with the PQQ-GDH reaction. For this purpose, mutarotase was added in the enzyme solution. Under such conditions, the i_{lim} reached a constant value within 15 min. Furthermore, the steady-state value of i_{lim} is accounted for 161% of that in the absence of mutarotase (at 15 min). The value is very good agreement with the concentration ratio of the total glucose against β-D-glucose in mutarotative equilibrium. These results indicate that the complete redox conversion of the total glucose to hydroquinone is successfully achieved under the present conditions.

The i_{lim} for the glucose determination showed a linear relationship against *c*(glucose) with correlation coefficients larger than 0.998. The relative standard deviation for five independent measurements was 1.2% at *c*(glucose) = 5.0 mM with the MEA (*N* = 7).

The sensitivity (= 4*NnFrD*) was 4.0×10^{-2} A M^{-1} for *N* = 7, 1.8×10^{-2} A M^{-1} for *N* = 3, and 5.7×10^{-3} A M^{-1} for *N* = 1. By considering that *n* = 2 in this case, the average value of 4*FrD* is evaluated as 2.8×10^{-3} A M^{-1}. The value is in good agreement with that (2.8×10^{-3} A M^{-1})

evaluated from separate experiments on i_{lim} of hydroquinone in the same buffer solution containing the enzymes.

4. Conclusion

The diffusionally independent MEA electrode proposed here gives very stable and reproducible i_{lim}. Once the conditional parameter $4NnFrD$ is estimated, the bulk concentration of analyte can be easily determined from i_{lim} within a few seconds. The amperometric method can be successfully combined with endpoint enzyme assays using mediated bioelectrocatalysis, in which i_{lim} of the mediator generated in the enzyme reaction was determined with the MEA. The principle is applicable to almost all redox enzymatic assays, including micro-plate analysis. Selection of better mediator will improve the proposed method into the practical use level.

References

1. B.J. Privett, H.S. Jae, M.H. Schoenfisch, Anal. Chem., 80 (2008) 4499-4517.
2. B. Limoges, J. Moiroux, J.-M. Savéant, J. Electroanal. Chem. 521 (2002) 1-7.
3. W.J. Albery, P.N. Bartlett, J. Electroanal. Chem. 194 (1985) 211-222.
4. M. Fukaya, H. Ebisuya, K. Furukawa, S. Akita, Y. Kawamura, S. Uchiyama, Anal. Chim. Acta 306 (1995) 231-236.
5. S. Tsujimura, A. Nishina, Y. Kamitaka, K. Kano, Anal. Chem., 81 (2009) 9383-9387.
6. K. Aoki, Electroanalysis, 5 (1993) 627-639.
7. O. Ordeig, J. del Campo, F.X. Muñoz, C.E. Banks, R.G. Compton, Electroanalysis 19 (2007) 1973-1986.
8. X.-J. Huang, A.M. O'Mahony, R.G. Compton, Small 5 (2009) 776-788.
9. T.J. Davies, S. Ward-Jones, C.E. Banks, J. del Campo. R. Mas, F.X. Muñoz, R.G. Compton, J. Electroanal. Chem, 585 (2005) 51-62.

10. T.J. Davies, R.G. Compton, J. Electroanal. Chem, 585 (2005) 63-82.
11. D. Menshykau, X.J. Huang, N.V. Rees, F.J. del Compo, F.X. Muñoz, R.G. Compton, Analyst, 134 (2009), 343-348.
12. Y. Saito, Rev. Polarogr. 15 (1968) 177-186.
13. N. Fujieda, N. Tsuse, A. Satoh, T. Ikeda, K. Kano, Biosci. Biotechnol. Biochem. 69 (2005) 2459-2462.
14. M.A. Beaven, A. Robinson-White, N.B. Roderick, G.L. Kauffman, Klin. Wochenschr. 60 (1982) 873-881.
15. L. Lehane, J. Olley, Int. J. Food Microbiol. 58 (2000) 1-37.
16. M. Tsutsumi, N. Fujieda, S. Tsujimura, O. Shirai, K. Kano, Biosci. Biotechnol. Biochem. 72 (2008) 786-796.
17. R. Yamada, N. Fujieda, M. Tsutsumi, S. Tsujimura, O. Shirai, K. Kano, Electrochemistry 76 (2008) 600-602.
18. K. Takagi, S. Shikata, Anal. Chim. Acta 505 (2004) 189-193.
19. M. Niculescu, I. Frébort, P. Peč, P. Galuszka, B. Mattiasson, E. Csöregi, Electroanalysis 12 (2000) 369-375.
20. M.G. Loughran, J.M. Hall, A.P.F. Turner, V.L. Davidson, Biosens. Bioelectron. 10 (1995) 569-576.
21. J. Wang, Chem. Rev. 108 (2008) 814-825.
22. L. Ye, M. Hämmerle, A.J.J. Olsthoorn, W. Schuhmann, H.-L. Schmidt, J.A. Duine, A. Heller, Anal. Chem., 65 (1993) 238-241.
23. N. Okumura, T. Abo, S. Tsujimura, K. Kano, Electrochemistry 74 (2006) 639-641.

Figure Captions

Fig. 1. (a) Schematic diagram of the integration process, (b) the photo image and (c) the

224 structure of MEA.

225

226 Fig. 2. Cyclic voltammograms obtained at MEA with *N* = (a) 1, (b) 3 and (c) 7 for 1 mM
227 $[Fe(CN)_6]^{3-}$ in 1 M KCl, at a scan rate 20 mV s^{-1}. Inset: chronoamperometric responses for
228 $[Fe(CN)_6]^{4-}$ in 1 M KCl in potential step from –0.1 V to +0.6 V at MEA (*N* = 1, 3, 7 from
229 bottom to top).

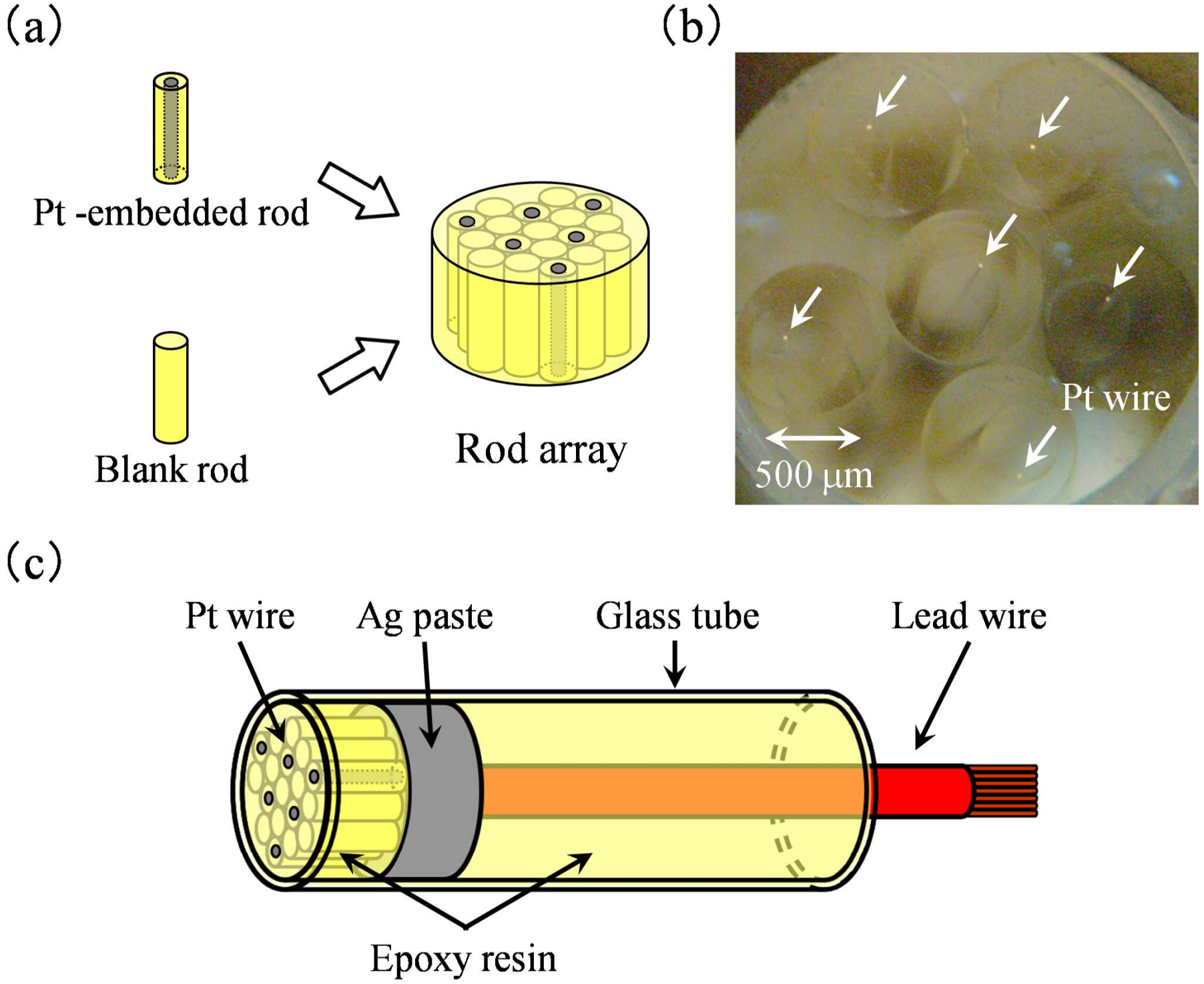
(a)
Pt -embedded rod
Blank rod
Rod array
(b)
Pt wire
500 μm
(c)
Pt wire
Ag paste
Glass tube
Lead wire
Epoxy resin

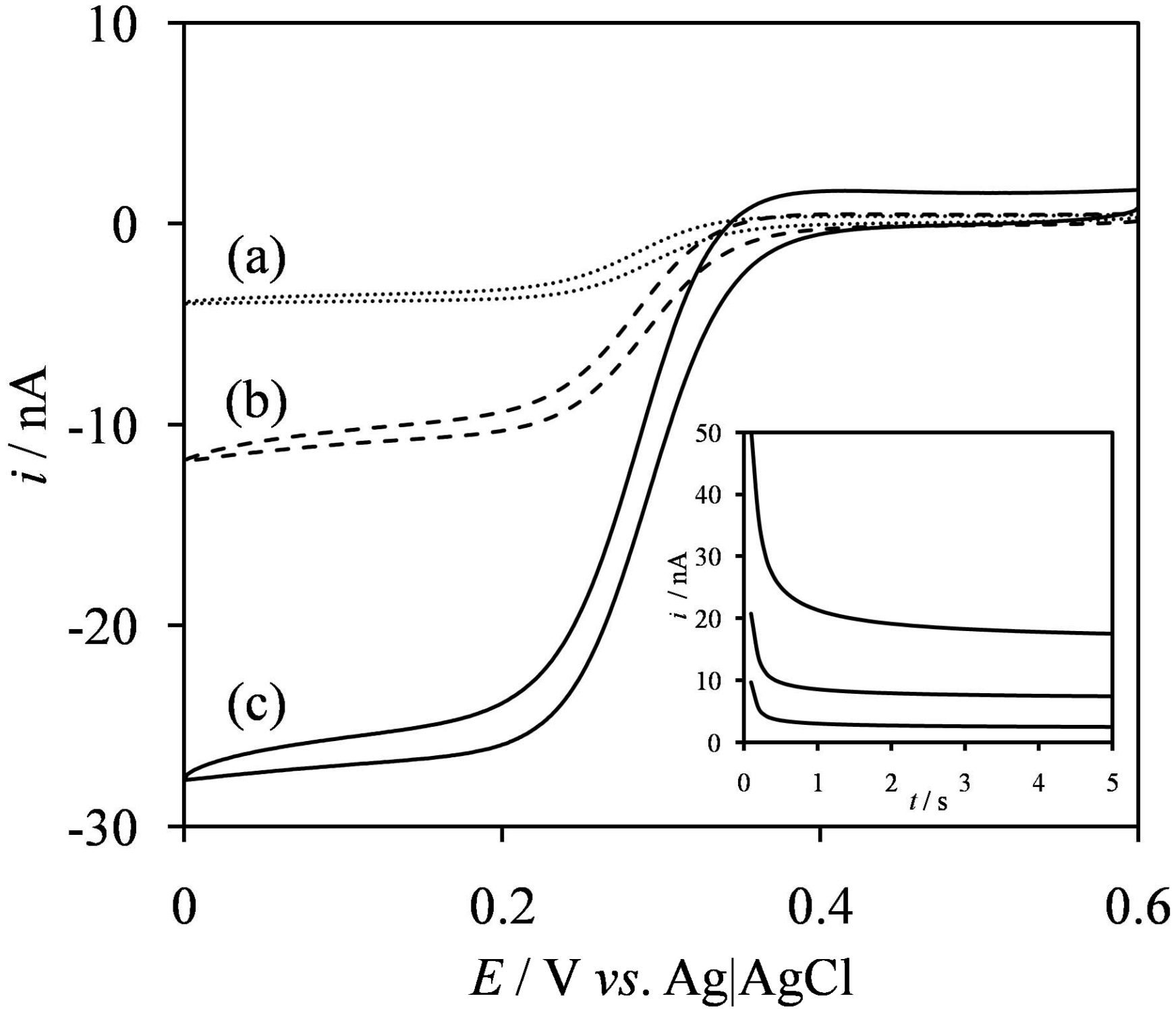
10
0
-10
-20
-30
i / nA
(a)
(b)
(c)
0
0.2
0.4
0.6
E / V vs. Ag|AgCl
50
40
30
20
10
0
i / nA
0
1
2
3
4
5
t / s